JOURNAL OF THE ROYAL SOCIETY INTERFACE

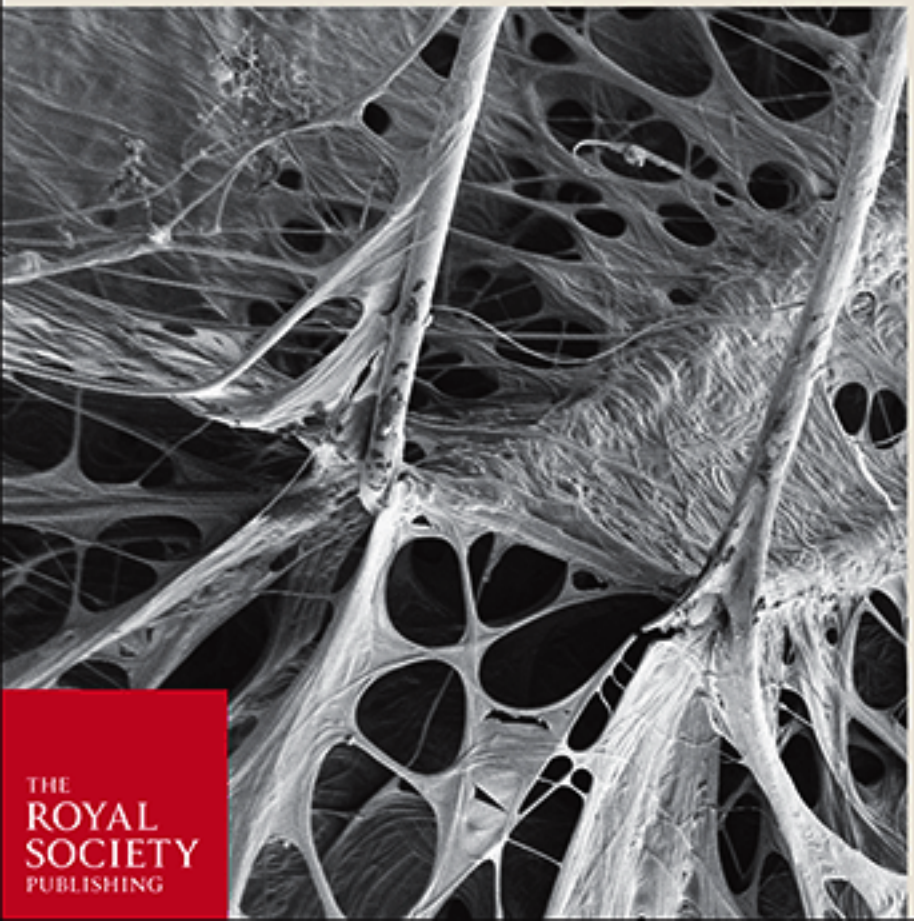

THE ROYAL SOCIETY PUBLISHING

INTERFACE

royalsocietypublishing.org/journal/rsif

Research

Cite this article: Greco G, Pugno NM. 2021 How spiders hunt heavy prey: the tangle web as a pulley and spider's lifting mechanics observed and quantified in the laboratory. *J. R. Soc. Interface* **18**: 20200907.
https://doi.org/10.1098/rsif.2020.0907

Received: 9 November 2020
Accepted: 12 January 2021

Subject Category:
Life Sciences–Engineering interface

Subject Areas:
biomechanics

Keywords:
spider silk, Theridiidae, biomechanics, mechanical properties, spider's behaviour

Author for correspondence:
Nicola M. Pugno
e-mail: nicola.pugno@unitn.it

Electronic supplementary material is available online at https://doi.org/10.6084/m9.figshare.c.5287602.

THE ROYAL SOCIETY PUBLISHING

How spiders hunt heavy prey: the tangle web as a pulley and spider's lifting mechanics observed and quantified in the laboratory

Gabriele Greco[1] and Nicola M. Pugno[1,2]

[1]Laboratory of Bio-inspired, Bionic, Nano, Meta Materials and Mechanics, Department of Civil, Environmental and Mechanical Engineering, University of Trento, Via Mesiano, 77, 38123 Trento, Italy
[2]School of Engineering and Material Science, Queen Mary University of London, Mile End Road, London E1 4NS, UK

GG, 0000-0003-3356-7081; NMP, 0000-0003-2136-2396

The spiders of Theridiidae's family display a peculiar behaviour when they hunt extremely large prey. They lift the quarry, making it unable to escape, by attaching pre-tensioned silk threads to it. In this work, we analysed for the first time in the laboratory the lifting hunting mechanism and, in order to quantify the phenomenon, we applied the lifting mechanics theory. The comparison between the experiments and the theory suggests that, during the process, spiders do not stretch the silk too much by keeping it in the linear elastic regime. We thus report here further evidence for the strong role of silk in spiders' evolution, especially how spiders can stretch and use it as an external tool to overcome their muscles' limits and capture prey with large mass, e.g. 50 times the spider's mass.

1. Introduction

Spiders exhibit a large variety of behaviours [1] and, in this context, the ability to use silks has evolved over almost 400 Myr to fulfil various functions [2] such as building webs [3] or cocoons [4], for courtship or ballooning [5]. For these reasons, most spider silks have high tensile strength, extensibility and toughness [6,7], as well as a strong stiffening at high deformations, which has recently been even observed by Brillouin light scattering experiments [8,9]. Among all the functions that are achieved through silk, prey capture with webs has always intrigued scientists. As an example, the efficiency of orb webs in stopping flying prey requires high mechanical performances of the webs, which both absorb kinetic energy [10] and minimize the damage after impact [9]. Interestingly, spider silks and webs can also act as external power amplifiers because of the elastic energy stored in the material and structure. For example, the spider *Hyptiotes cavatus* stretches its web by tightening an anchor line over multiple cycles of limb motion, and then releases its hold on the anchor line when an insect strikes the web, which rapidly tangles it [11]. This is a quite rare feature in animals that commonly store the elastic energy in the organisms' own anatomical structures [12–18]. Another example of external power amplification could be given by the fascinating hunting behaviours of theridiid spiders (figure 1*a*). These spiders use the particular structure of the cobweb, which has gumfoot threads that run from the substrate to the main frame [19]. These threads are easily detached from the substrate when disturbed by walking prey and thus release the elastic energy stored in the main frame of the web [20]. Consequently, if the prey is small (e.g. ant [21]), the gumfoot threads yank it upwards. In this way, small animals become suspended helplessly in the air. With the increase in the prey dimensions, it may happen that more than one single gumfoot thread is involved in the suspension. More commonly, bigger sized preys are not completely lifted by a single thread, and theridiid spiders usually rush down and immobilize such prey using aciniform (wrapping) silk.

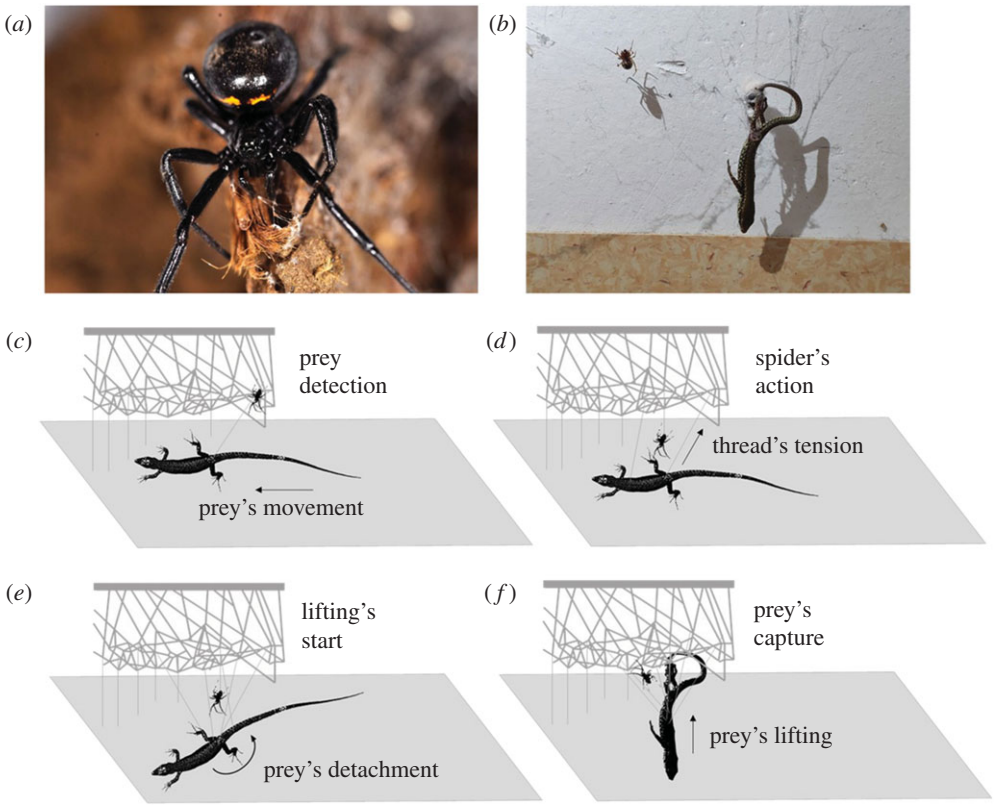

Figure 1. (*a*) An adult *Steatoda paykuliana* female of the family of Theridiidae (courtesy of Alessandro Kulczycki, Aracnofilia – The Italian Association of Arachnology). (*b*) A *Steatoda triangulosa* that captured a lizard (*Podarcis muralis*) by using lifting technique (courtesy of Emanuele Olivetti). Schematic of the technique used to lift the prey. (*c*) The prey is detected by the capturing threads and, once it is, (*d*) the spider starts to attach pre-tensioned threads to it. (*e*) When the weight of the prey is won by vertical component of the sum of the tensions the prey detaches from the surface and (*f*) starts to be lifted.

In both these cases (likely the majority of hunt events in nature) spiders carry the prey back to the retreat on their spinnerets, as seen in practically all web spiders. On the other hand, if the prey is extremely large compared to the spider (figure 1*b*), it poses extreme challenges (with a large nutritional reward), and a different hunting behaviour, involving the investigated lifting mechanism, is displayed.

Once the large walking prey is attached to a capture sticky thread [22,23] of the three-dimensional cobweb (figure 1*c*), the spider lifts it through sequential addition of pre-stretched silk threads produced by major ampullate gland [24] (figure 1*d–f*). Between the addition of two threads, the aciniform silk and the venom are also used to further immobilize the prey. Again, the lifting prevents prey from escaping their web since it can no longer hold on to the underlying surface. Several records show that small reptiles and mammals are occasionally captured in this way [25,26]. The first records published were the cases of a snake (about 55 g) and a mouse that were not able to move and escape because they were lifted off the ground [27]. Interestingly, during prey capture those spiders were continuously moving upward and downward with respect to the prey. This one was gradually lifted to a certain height (more than 10 cm). A subsequent more accurate description revealed that the spider attached to the animal silk threads and their length gradually decreased while the mouse was lifted [24]. McKeown [28] associated this mechanism to the one used by other spiders (such as *Cyrtophora* sp., *Olios* sp. and *Phonognatha* sp.) to lift inanimate objects, e.g. leaves or empty shells that are typically used as a temporary den [29–32]. Decary [33] observed that this lifting mechanism allows spiders of the genus *Olios* sp. [34] to lift snail shells that are more than 35 times the mass of the animal. As in theridiid spiders, *Olios coenobita* attaches silk threads, gradually shorter in length, to the object to apply a sum of tensions used to counteract gravity. Fage [34] suggested that the lifting of small stones in orb webs was due to the elastic silk threads, and not done by the muscle power of the spider. The spider lifting (and dragging) mechanics was theoretically described by Pugno [35] who also showed how the natural (e.g. nonlinear) behaviour of the spider silk improves the efficiency of the lifting.

In this work, we studied experimentally for the first time the lifting mechanics used to hunt extremely large prey displayed by spiders of the family Theridiidae. To explain the phenomenon, we compared the experiments with the predictions of the theoretical model (here adapted) [35]. The results are another example of the efficiency of the spiders in using silk and their web as external tools (i.e. like a pulley) that allow them to perform actions that would be impossible simply by using their muscles. Moreover, with the support of the mechanical model, we find that spiders apparently do not overstretch the silk threads used in the hunt. The lifting mechanism is, thus, another good example of the central role of silk in spider's evolution.

2. Material and methods

2.1. The mechanical model

In order to rationalize the lifting observations, we apply the lifting mechanics theory developed by Pugno [35] (for the equations we refer to figure 2).

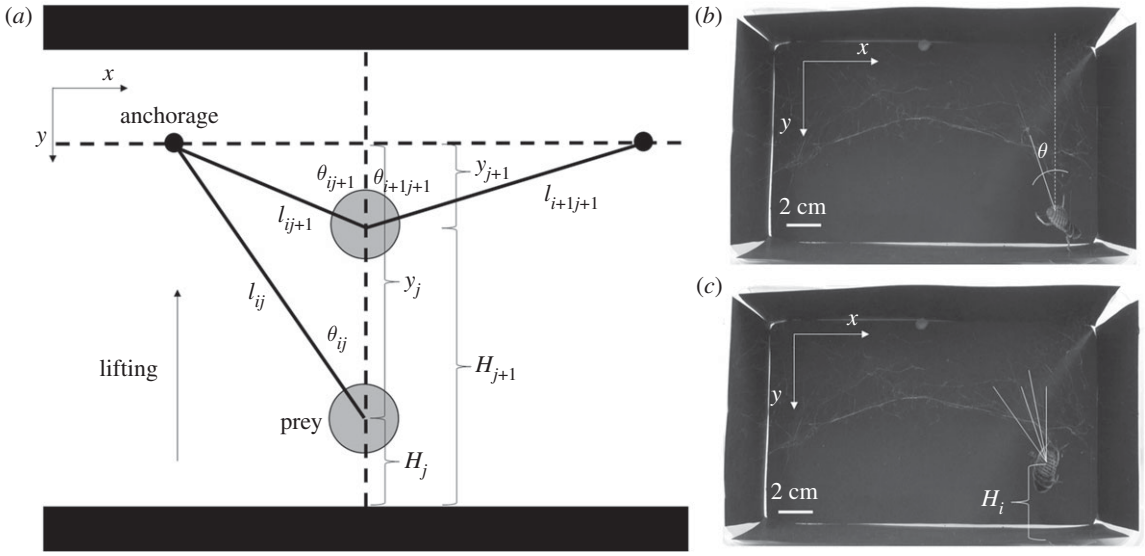

Figure 2. (*a*) Schematic of the lifting process. (*b*) First step of the lifting process with the frame. (*c*) After several steps the prey is lifted and the final height is H_i. This is achieved by using various threads.

At each step, the spider adds a thread, with a cross section area A, and the prey moves (if it does) until an equilibrium position. The vertical equilibrium is achieved through the sum of the vertical components of the threads' tensions that balance the weight of the prey. The horizontal equilibrium is achieved through the sum of the horizontal's components of the threads' tensions. For the sake of simplicity, we neglect the (nearly) horizontal threads only responsible for the horizontal equilibrium, which is here considered satisfied by definition.

The lifting of the prey did not occur immediately after the insertion of the first thread. In fact, only after a given number (N_I) of attached threads the prey started to be lifted. Then the count of the lifting's steps (j) started: only these N_{I+j} were considered in the vertical equilibrium of the suspended prey. We named the weight of the prey W, the thread number with the index i and the lifting's step with the index j.

As suggested in Pugno [35], we considered two lifting strategies: all the inserted threads had the same unstretched length l_{i0} (first strategy, $l_{i0} = l_0$) or after the insertion of the l_{ij} all threads changed tension in order to reach the same level of strain ε_j (second strategy). Since spider silk presents an initial linear elastic regime and a subsequent nonlinear elastic regime (electronic supplementary material, figure S1), we considered the situation of small deformations (linear regime) and large deformations (nonlinear regime). For the former, we used the following constitutive law

$$\sigma = E\varepsilon,$$

where E is Young's modulus of the silk and ε its deformation. We used the following relationship between ε and the initially inserted (l_{ij}) and undeformed (l_{i0}) lengths of the threads

$$\varepsilon_{ij} = \frac{l_{ij}}{l_{i0}} - 1.$$

The nonlinear geometrical and constitutive regime were described by the following nonlinear constitutive law [35]

$$\sigma_{ij} = \frac{\sigma_u}{\varepsilon_u^\alpha} \ln^\alpha \left(\frac{l_{ij}}{l_{i0}}\right),$$

where σ_u is the ultimate strength of the silk, ε_u is the ultimate strain and α describes the power of the constitutive law: $\alpha = 1$ linear elasticity (in the limit of small strains), $\alpha > 1$ stiffening behaviour (commonly observed in natural material such as silk), $0 \leq \alpha < 1$ softening (usually observed in engineering materials).

The purpose of the lifting hunt mechanism is to avoid the prey escaping thanks to the lifting. For this reason, what matters the most is the vertical component of the motion of the prey.

2.1.1. Linear regime I strategy

Following figure 2, we wrote the vertical force equilibrium between the weight of the prey and the overall vertical component of the tension generated by the threads for each lifting's step (see electronic supplementary material). Then, following [35], we worked out the height of the prey at step n as a function of the measured thread angles (θ_{in}, figure 2*a*)

$$\begin{aligned} H_n &= y_0 - y_n \\ &= y_0 - \frac{l_0}{E(N_I + n)} \left(\frac{W}{A} + E \sum_{i=1}^{N_I} \cos\theta_{in} + E \sum_{i=1}^{n} \cos\theta_{in} \right). \end{aligned} \tag{2.1}$$

2.1.2. Linear regime II strategy

In this case, the length l_0 was not known but the overall strain of all the threads at each step j was known (ε_j). Again, we analysed step by step (see electronic supplementary material) and thus obtained the height of the prey at step n as

$$\begin{aligned} H_n = y_0 &- \frac{1}{E(1+\varepsilon_n)} \left(\frac{W}{A} + E \left(\sum_{i=1}^{N_I} \cos\theta_{in} + \sum_{i=1}^{n} \cos\theta_{in} \right) \right) \\ &\times \left(\sum_{i=1}^{N_I} \frac{1}{l_{in}} + \sum_{i=1}^{n} \frac{1}{l_{in}} \right)^{-1}. \end{aligned} \tag{2.2}$$

2.1.3. Nonlinear regime II strategy

For the sake of simplicity, we did not consider the I strategy for the nonlinear regimes.

Following the previous logic and the process step by step (see electronic supplementary material, information), we computed the height at step n

$$H_n = y_0 - \frac{W}{A} \frac{\varepsilon_u^\alpha}{\sigma_u} \frac{1}{\ln^\alpha(1+\varepsilon_n)} \left(\sum_{i=1}^{N_I} \frac{1}{l_{in}} + \sum_{i=1}^{n} \frac{1}{l_{in}} \right)^{-1}. \tag{2.3}$$

2.1.4. Process efficiency

An efficiency was associated with the lifting process. In particular, a step efficiency is calculated as [35]

$$\eta = \frac{1}{n + N_I}, \tag{2.4}$$

and a gravitational efficiency (energetic efficiency) defined by Pugno [35] as following:

$$\eta' = \frac{WH}{N_I wH + w\sum_{i=1}^{j} y_i}, \tag{2.5}$$

where w was the weight of the spider and H was the final height. The lifting velocity was calculated as

$$V = \frac{H}{t}, \tag{2.6}$$

where t was the time of the whole process.

2.1.5. Input parameters for the model

We used experimental values and we inserted them in equations (2.1)–(2.3) by means of some assumptions. The parameters inserted in equations (2.1)–(2.3) (i.e. E, σ_u, ε_u, α and A) were estimated through the measure of the mechanical properties of the supporting threads (lifting threads produced by major ampullate gland). The lengths and the angles of the threads were measured by means of the recorded videos. For the parameter α, we extrapolated it by fitting the nonlinear regions of the stress–strain curves (electronic supplementary material, figure S1). Since it was impossible to measure l_{i0}, we calculated it using

$$\varepsilon = \frac{l_{ij}}{l_{i0}} - 1,$$

where for ε we assigned two constant characteristic plausible values: one characteristic of the linear elastic regime and the other of the nonlinear one, respectively, 0.05 and 0.25. By fitting the model, we were able to see which kind of constitutive law regime was more representative for the silk during the lifting and possibly which strategy was preferred.

2.2. Spiders, their cages and prey

The spiders under study belonged to the family of Theridiidae. We used five animals: one *Steatoda paykulliana* and four *Steatoda triangulosa*. All of these animals were kept in plastic boxes covered with black paper inside at room temperature (20–23°C and 30–39% RH) (figure 2*b*,*c*). This was done to highlight the contrast between the silk of the webs and the surrounding and thus facilitate the measurements of the thread lengths and geometry. The selected prey was *Blaptica dubia*, a cockroach from Central and South America. This was selected since its strength and weight are 2-50 times higher with respect to the spiders. In this context, the lifting of this animal represents a challenge for the spiders under study. Each animal was weighted before the test with a high-resolution scale.

2.3. Silk mechanical properties

From the cobwebs, we cut the trapping thread above the region covered with glue droplets. Then, we glued (with a double side tape) the silk samples on a paper frame provided with a square open window of 1 cm side. For tensile tests, we used a nanotensile machine (Agilent technologies T150 UTM) with a cell load of 500 mN. The applied strain rate was 1%/s. We computed the engineering stress dividing the measured force by the cross-sectional area of each tested thread. The diameter of the fibres was measured with the support of a light microscope [36], and the cross-sectional area of the thread (which can be composed of more fibres) was calculated using the sum of the fibres cross-sectional area. We present the data with the mean value and standard deviation. For *Steatoda paykulliana*, we measured 10 samples of silk. For *Steatoda triangulosa* 32 (eight for each animal).

2.4. Scanning electron microscopy

A FE-SEM (Zeiss-40 Supra) was used to investigate the morphology of the web's junctions and threads. We used a Zeiss –40 Supra. The metallization was made by using a sputtering machine Quorum Q150T and the sputtering mode was Pt/Pd 80:20 for 5 min.

2.5. Measure of the thread length

The lifting predation was recorded with a high-resolution Sony camera. In order to estimate the silk thread length and the height of the prey, we stopped the video when the spider attached the thread to the prey and measured the length and the angles through the support of ImageJ software analysis [37] (figure 2*b*,*c*). Each parameter was measured five times and its mean value and standard deviation computed; then we used the average for the fit. All the threads lengths and angles as well as their uncertainties are reported in electronic supplementary material, data sheet. Among all the attempts in filming the lifting mechanism, we selected the best five videos (see electronic supplementary material, videos), where these were the only ones that allowed us to perform the previous mentioned quantitative analysis.

At each step, in this way, we had the static situation in an equilibrium point (measures of the threads' lengths, their inclination, and anchorages' threads heights) that was used to apply the theoretical model.

3. Results

3.1. Structure of the webs

The structure of the 3D cobweb was complex as depicted in figure 3*a*. However, some of the web's components could easily be identified. With the supporting threads (figure 3*b*), the spider produced the main structure of the web (upper part) and it protected the den by creating a shell of these threads in the frontal part of the web [19,39,40]. In order to join two or more of these threads, piriform and aggregate silks were used (figure 3*f*) to create strong junctions [22,41]. Moreover, the spiders of the family Theridiidae used aggregate silk to cover capture threads with glue [42]. The threads were fixed to the surfaces by means of attachment discs produced by the piriform silk (figure 3*d*,*e*) [43,44]. In all cases, the spiders under analysis built the webs with the capture threads near the bottom of the enclosure.

3.2. Mechanical properties of the silk

Electronic supplementary material, figure S2 and table 1 show the mechanical properties of the major ampullate silk (extracted from supporting threads) of the spiders that were studied. The typologies of fibres are two: one for the species *S. paykulliana* and one for *S. triangulosa*. We chose this type of silk because it is supposed to be used during the lifting [35]. The silks that were analysed presented remarkable mechanical properties, comparable to those reported in the literature [45]. The species of analysed spiders were *Steatoda triangulosa* and *Steatoda paykulliana*. Respectively, the measured strengths were 205 ± 106 MPa and 409 ± 356 MPa. The strain at break was, respectively, 0.42 ± 0.13 and 0.26 ± 0.15. Young's modulus was, respectively, 1.7 ± 1.5 GPa and 3.9 ± 3.3 GPa. The toughness modulus was, respectively, 50 ± 39 MJ m^{-3} and 49 ± 41 MJ m^{-3}. The α parameter was, respectively, 1.5 ± 0.5 and 1.2 ± 0.2. By considering the aim of our analysis, we were interested in the ultimate stress (σ_u, i.e.

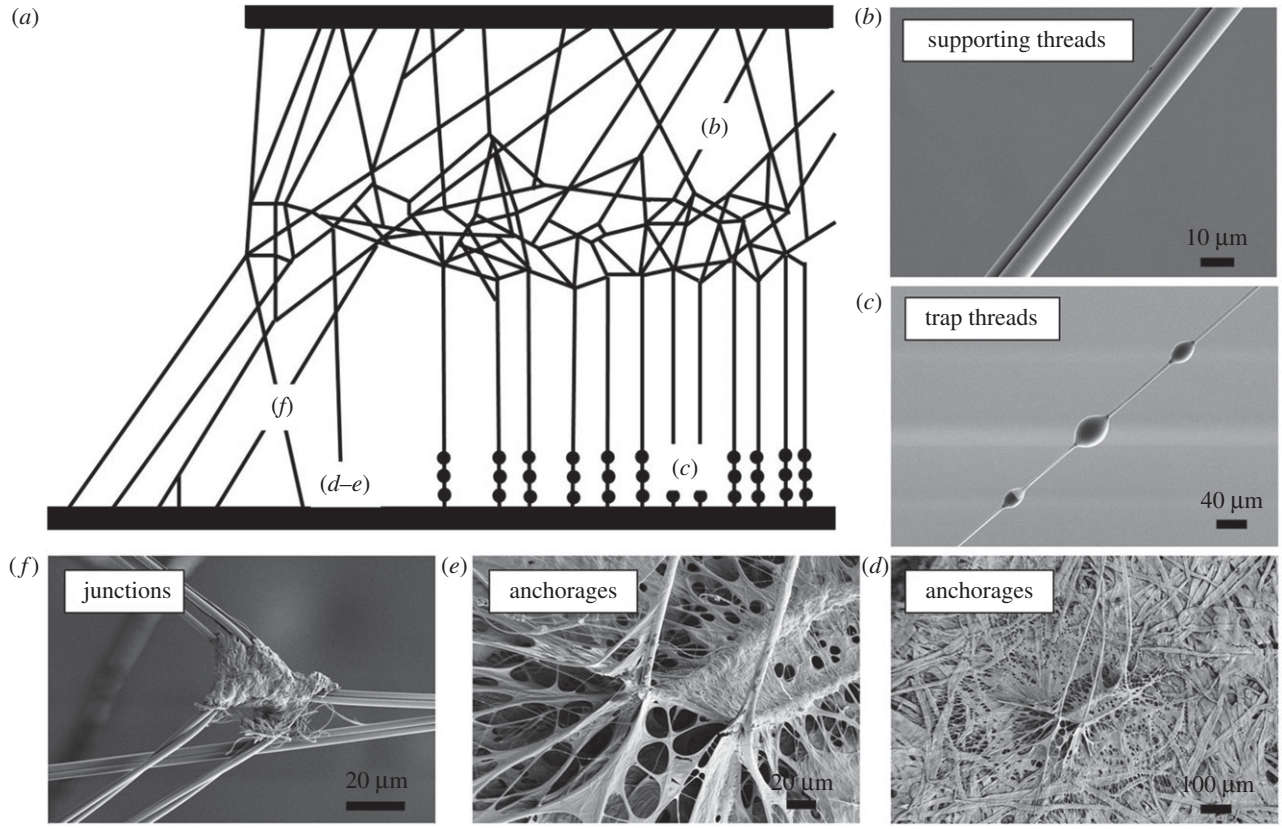

Figure 3. (*a*) Typical structure of a cobweb produced by the spiders of the family Theridiidae (adapted from [38]). (*b*) Supporting threads are produced mainly by using the major ampullate gland. (*c*) Trapping threads of the web placed close to the ground in order to catch the prey. The glue is produced by the aggregate gland and the main thread by the major ampullate gland. (*d*) The anchorage of the webs with the paper and (*e*) a detail of the anchorage. (*f*) Junctions that connect different frame threads on the web produced by the piriform and aggregate glands.

Table 1. The mechanical properties of the catching thread (without glue) of the two species of spiders studied.

species	no. samples	fibre diameter (µm)	strain at break	strength (MPa)	Young's modulus (GPa)	toughness modulus (MJ m^{-3})	alpha α
Steatoda triangulosa	32	5 ± 2	0.42 ± 0.13	205 ± 106	1.7 ± 1.5	50 ± 39	1.5 ± 0.5
Steatoda paykuliana	10	7 ± 2	0.26 ± 0.15	409 ± 356	3.9 ± 3.3	49 ± 41	1.2 ± 0.2

strength) and ultimate strain (ε_u) that were inserted in equations (2.1)–(2.3). Thus, we used the obtained mean values of these parameters for the application of the theoretical model to our experimental set-up. In particular, for *Steatoda triangulosa* $\varepsilon_u = 0.42$ and $\sigma_u = 205$ MPa were used, whereas for *Steatoda paykulliana* $\varepsilon_u = 0.26$ and $\sigma_u = 409$ MPa were used. Moreover, the cross-sectional area A was computed by summing the cross-sectional area of the fibres that composed the thread (usually 2–3), which were computed using the mean value of the fibres diameters (table 1). Furthermore, in the equations the parameter $\varepsilon_n = \varepsilon = \text{const.}$ is present, which defines the strain of the inserted thread. Up to the model that we considered, i.e. large or small deformations, the values associated to this parameter were different. In particular, for *Steatoda paykulliana* we used $\varepsilon = 0.15$ and $\varepsilon = 0.05$, respectively; and for *Steatoda triangulosa* we used $\varepsilon = 0.25$ and $\varepsilon = 0.05$, respectively. These parameters were chosen on the basis of the related stress–strain curves as representative of large or small deformations. In this regard, for large deformation we considered the middle part of the second stiffening phase as the level of strain of the inserted fibre. For small deformation, on the other hand, we chose the mean value of the yielding point.

3.3. The lifting

During the predation, the spiders displayed different behaviours, which can be due to the fact that the prey were alive and this affected the observation.

In all the five selected videos (see supporting videos) when the spiders reached the prey, they started to wrap it with aciniform silk [46]. Moreover, when the prey reached the main frame of the tangle web, the lifting was strongly affected by the presence of numerous obstacles, i.e. frame threads. In this context, we observed that the spiders somehow removed these obstacles. For the fourth sample the prey climbed the wall of the cage for a few centimetres. The lifting occurred when it fell down and the spider started to wrap it.

Table 2. The efficiencies and velocities of the lifting of the different cases analysed in this study. η indicate the process' efficiency and η' indicate the gravitational efficiency and V the lifting velocity.

spider	mass of the spider (g)	mass of the *Blaptica dubia* (g)	η	η'	V (cm s^{-1})
Steatoda triangulosa I	0.14 ± 0.01	0.31 ± 0.01	0.04	0.11	0.0046
Steatoda triangulosa II	0.04 ± 0.01	0.34 ± 0.01	0.02	0.06	0.0021
Steatoda triangulosa III	0.02 ± 0.01	0.34 ± 0.01	0.03	0.08	0.0039
Steatoda triangulosa IV	0.01 ± 0.01	0.50 ± 0.01	0.03	0.32	0.0117
Steatoda paykulliana	0.22 ± 0.01	0.36 ± 0.01	0.06	0.08	0.0007

To calculate the vertical distance between the anchorage and the prey (namely y_j), we measured the length of the inserted thread and the (cosine of the) angle between the thread and the vertical axes (figure 2). All the lengths and angles values as well as their uncertainties are reported in the electronic supplementary material, data sheets. The height H_j of the prey is the distance between the cockroach and the ground level. These measurements were performed for each set of threads for all taken videos.

In all the cases, the lifting did not occur immediately after the insertion of the first thread. On the other hand, they started after N_I threads, which are listed in electronic supplementary material, table S1. During the predation behaviours, as depicted in electronic supplementary material, figure S3, the inserted fibres were all different in terms of lengths for all the spiders and no apparently regularity was observed (for the values and the uncertainties see electronic supplementary material, data sheet). In this regard, electronic supplementary material, table S1 shows the number of threads used to lift the prey ($n + N_I$, which was considered in the theoretical model), their mean length and the final height reached by the prey. For the cases under study, i.e. *Steatoda triangulosa* I, *Steatoda triangulosa* II, *Steatoda triangulosa* III, *Steatoda triangulosa* IV and *Steatoda paykulliana* we observed, respectively, $n + N_I$ equal to 29 ($N_I = 5$), 73 ($N_I = 13$), 47 ($N_I = 11$), 34 ($N_I = 3$) and 17 ($N_I = 13$). Respectively, the masses of the spider (and prey) were 0.14 ± 0.01 g (0.31 ± 0.01 g), 0.04 ± 0.01 g (0.34 ± 0.01 g), 0.02 ± 0.01 g (0.34 ± 0.01 g), 0.01 ± 0.01 g (0.50 ± 0.01 g) and 0.22 ± 0.01 g (0.36 ± 0.01 g). Furthermore, it is interesting to note the final height of the lifted prey. Comparing it with respect to the height profile of the tangle web main structure (electronic supplementary material, figure S4) it is possible to notice that the final height was quite close to the height profile of the main structure, but not higher. In particular, the final heights that we detected were, respectively, 5.70 ± 2.39 cm, 4.30 ± 2.07 cm, 3.00 ± 1.73 cm, 5.40 ± 2.30 cm, 0.80 ± 0.35 cm (electronic supplementary material, table S1). The reason for this could be the dense net of silk fibres in the main frame of cobwebs, which obstructed the lifting.

During lifting, spiders used different anchorages where they secured the threads. Equations (2.1)–(2.3) require that the value of the anchorages' height is constant. In electronic supplementary material, figure S5 the measured height of the anchorages and the height of the prey are depicted and it is possible to see that the height of the anchorages did not change considerably during the process.

The predation was considered finished when the spiders stopped its lifting activity.

3.4. The mechanics of lifting: theory compared to experiments

To compare the experimental and theoretical results we neglected, for the sake of simplicity, the viscoelastic relaxation of the silk. This could be considered a reasonable ansatz since the low timing of the lifting, i.e. approximately 10 min.

We have analysed the lifting mechanics firstly by considering the real efficiency described in equation (2.4) and with the gravitational efficiency described in equation (2.5). Moreover, the mean lifting velocity has been associated with every lifting experiment (equation (2.6)). Table 2 shows the values of these parameters and also the mass of the spiders and the cockroaches that were lifted.

In particular, the spider that showed the highest absolute efficiency η was *Steatoda paykulliana* (0.06). On the other hand, *Steatoda triangulosa* presented comparable values (namely 0.04, 0.02, 0.03, 0.03). In term of gravitational efficiency, the obtained values were more inhomogeneous, and respectively we obtained 0.11, 0.06, 0.08, 0.32 and 0.08. The fourth spider had the highest gravitational efficiency because it was the spider that lifted, relatively, the heaviest prey. In particular, the weight of the quarry was 50 times the spiders. The slowest lifting process (lifting velocity, i.e. equation (2.6)) was that of *Steatoda paykulliana* (the lowest final height was observed for this spider). Respectively, the obtained velocities were 0.0046 cm s^{-1}, 0.0021 cm s^{-1}, 0.0039 cm s^{-1}, 0.0117 cm s^{-1} and 0.0007 cm s^{-1}.

To compare the theoretical model with the experimental data, we used equations (2.1)–(2.3). We firstly measured the mechanical properties of the spider silks involved. Then, at the end of each step (equilibrium state), we measured the threads length, their inclination and the height of the prey. The obtained data were inserted in the previously mentioned equations that were compared to the actual lifting experiments. The comparison among the theoretical models (i.e. linear regimes I and II, and nonlinear regime II) and the experimental data are depicted in figure 4 and electronic supplementary material, figure S6. The difference between the two strategies in the linear regimes was small and no major differences occurred. A discrepancy between the predicted linear models and the experimental values was noticed at high step number. This discrepancy (as well as the decrease in height) is due to the fact that in the theoretical model the experimental thread lengths and angles values were inserted. These are affected by uncertainties (see electronic supplementary material, data sheet) and thus our comparison is not a best fit.

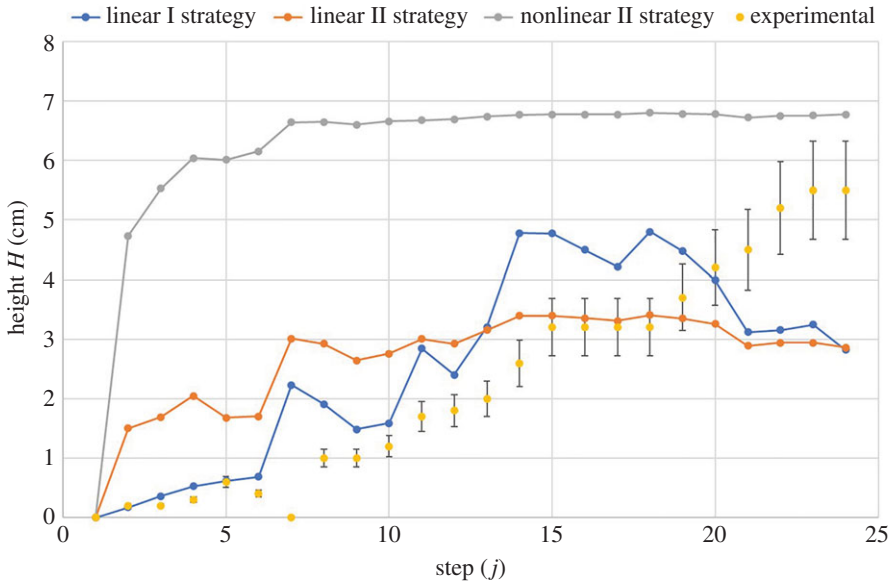

Figure 4. Representative comparison among the theoretical model and the experimental data of the lifting. Grey lines denote nonlinear elastic regime (II strategy); blue lines, linear elastic regime (I strategy); orange line, linear elastic regime (II strategy); yellow line, experimental data.

As highlighted in Pugno [35], the nonlinear regime improves the efficiency of the lifting especially in the first lifting steps. With the exception of the last case (*Steatoda paykulliana*), we noticed that the assumption of the linear regime of the silk agreed better with the experimental results. This means that *Steatoda triangulosa* did not stretch the silk's threads until large deformations and only the assumption of the linear regime was self-consistent with the experimental observations. It is possible that this occurs because silk threads deformed and kept in the linear elastic regimes are better in bearing loads cycles, with a small hysteresis [47–50]. This is beneficial for hunting mechanisms that involved extremely large prey that usually do not die immediately and, thus, fight for their lives.

4. Discussion and conclusion

Some spiders lift objects, to build dens [29,31,32,34], and to capture prey [20,21,25]. Theridiid spiders (figure 1*a*) are able to catch prey much larger and stronger than themselves (e.g. small lizards, small mammals or big insects) by lifting them and, thus, immobilizing them since they are unable to hold on to the underlying surface [24,25] (figure 1*b*). Whilst this mechanism is not used for small (medium) sized prey, which are lifted by using only the gumfoot threads and the elastic energy stored in it and in the related part of the cobweb [20,21,43], it represents an interesting example of how spiders are able to outperform their muscles limits. Nevertheless, in the case of extremely large prey, the elastic energy stored in the cobweb and the gumfoot threads may be not sufficient for the lifting and thus a multiple step lifting mechanisms is adopted.

In this work, we observed and quantified in the laboratory the lifting mechanism in its extreme condition, which was observed before only *in situ* and for inanimate objects [27]. The process requires the use of silk with good mechanical performances [6,7] (table 1) and the support of a robust 3D cobweb [20] (figure 3). In fact, by attaching pre-tensioned silk threads (probably produced by major ampullate gland), the spider is able to apply a sum of tension that overcomes the prey's weight (figure 1*c–f*). The lifting is not abrupt and it requires many steps, forcing the spider to continuously move upward and downward on the web. Also, the aciniform silk [46] as well as the venom are used to further immobilize the quarry during the process. This ended when the prey was close to the main frame of the tangle web, where the den of the spider lies but the dense network of silk fibres obstructs the movements of the quarry. This could be a reason why in the case of *Steatoda paykulliana* less steps and lower final heights were observed, since the main structure of its cobweb was particularly low (electronic supplementary material, figure S4). Moreover, since part of the cobweb (and not only the threads that are directly involved in the lifting) is indirectly involved in the hunt by releasing the related stored elastic energy [20], we do not exclude that a denser and larger mesh would improve the lifting mechanism. A comparison between the experimental results and the theoretical model of spider lifting mechanics [35] was performed under two main different hypotheses, i.e. small linear or large nonlinear deformations, suggesting that in our experiments the threads are working in nearly linear regime.

In the lifting of objects (such as shells or leaves or living prey), spiders may achieve higher lifting efficiency because of the nonlinear constitutive law of silk (i.e. large deformations) [35]. However, in our work with living prey, we observed that the linear strategy seems to be more compatible with the observations especially for *Steatoda triangulosa* (figure 4). Thus, the silk used during the lifting by these spiders is probably kept in the linear elastic regimes (i.e. small deformations) (electronic supplementary material, figure S1). In this way, the threads are able to recover and restore better the original deformations during loads cycles (due to the prey movement and lifting) [47,51]. Interestingly, this seems to counter the trend with respect to the passive hunting mechanisms of the orb webs [10], in which nonlinear behaviours are beneficial for both absorbing the kinetic energy of the prey and for reducing the damage in the web after the impacts [9].

Thus, it seems that Theridiid spiders are able to use the web and their silk as an external tool to hunt, which can be

tuned by the arachnid. In this context, the use of silk as an external tool to store elastic energy is not limited to Theridiid spiders. *Hyptiotes cavatus*, for example, uses its web as a power amplification to capture flying prey, which offers many advantages over the muscles limitations [11].

Although the experimental results are affected by large uncertainties as well as the theoretical model compare simple strategies, we provide the first quantitative observation in the lifting mechanisms of this spider for hunting living large preys. In conclusion, the spider lifting is emerging as another key mechanism of spiders that use naturally pre-stretched silk as an external tool (here like a pulley) to perform actions that are impossible only using their muscles. Thus, also for lifting, the silk threads seem to have a central role in spider's life and evolution.

Data accessibility. The authors declare that the data supporting the findings of this study are available within the article and its electronic supplementary material, information files.

Authors' contributions. G.G. performed the experiments, acquired the data and wrote the first draft of the paper. N.M.P. suggested the idea, supervised the work, helped with data analysis and in the writing of the manuscript. All authors viewed and approved the final manuscript and had the opportunity to comment on earlier drafts.

Competing interests. The authors declare that they have no competing interests.

Acknowledgements. G.G. and N.M.P. would like to thank Rainer Foelix for his comments and suggestions. G.G. would like to thank Victor Kang for his comments and suggestions and Matteo Colombo for the precious help in performing experimental activities as well as Luigi Lenzini for productive discussions. The authors would like to thank Lorenzo Moschini, Prof. Antonella Motta and Prof. Claudio Migliaresi (Biotech – Mattarello, University of Trento) for their support with the SEM facility. N.M.P. is supported by the European Commission under the FET Proactive (Neurofibres) grant no. 732344, the FET Open (Boheme) grant no. 863179 as well as by the Italian Ministry of Education, University and Research (MIUR) under the 'Departments of Excellence' grant L. 232/2016, the ARS01-01384-PROSCAN and the PRIN-20177TTP3S grants. G.G. is supported by this last grant.

References

1. Herberstein ME (eds). 2012 *Spider behaviour: flexibility and versatility*, 1st edn. Cambridge, UK: Cambridge University Press.
2. Brunetta L, Craig CL. 2012 *Spider silk evolution and 400 million years of spinning, waiting, snagging, and mating*. London, UK: Yale University Press.
3. Blackledge TA. 2012 Spider silk: a brief review and prospectus on research linking biomechanics and ecology in draglines and orb webs. *J. Arachnol.* **40**, 1–12. (doi:10.1636/M11-67.1)
4. Hakimi O, Knight DP, Knight MM, Grahn MF, Vadgama P. 2006 Ultrastructure of insect and spider cocoon silks. *Biomacromolecules* **7**, 2901–2908. (doi:10.1021/bm060528h)
5. Scott CE, Anderson AG, Andrade MCB. 2018 A review of the mechanisms and functional roles of male silk use in spider courtship and mating. *J. Arachnol.* **46**, 173–206. (doi:10.1636/JoA-S-17-093.1)
6. Agnarsson I, Kuntner M, Blackledge TA. 2010 Bioprospecting finds the toughest biological material: extraordinary silk from a giant riverine orb spider. *PLoS ONE* **5**, 1–8. (doi:10.1371/journal.pone.0011234)
7. Greco G, Pugno NM. 2020 Mechanical properties and Weibull scaling laws of unknown spider silks. *Molecules* **25**, 2938. (doi:10.3390/molecules25122938)
8. Wang Z, Cang Y, Kremer F, Thomas EL, Fytas G. 2020 Determination of the complete elasticity of *Nephila pilipes* spider silk. *Biomacromolecules* **21**, 1179–1185.
9. Cranford SW, Tarakanova A, Pugno NM, Buehler MJ. 2012 Nonlinear material behaviour of spider silk yields robust webs. *Nature* **482**, 72–76. (doi:10.1038/nature10739)
10. Sensenig AT, Lorentz KA, Kelly SP, Blackledge TA. 2012 Spider orb webs rely on radial threads to absorb prey kinetic energy. *J. R Soc. Interface* **9**, 1880–1891. (doi:10.1098/rsif.2011.0851)
11. Han SI, Astley HC, Maksuta DD, Blackledge TA. 2019 External power amplification drives prey capture in a spider web. *Proc. Natl Acad. Sci. USA* **116**, 12 060–12 065. (doi:10.1073/pnas.1821419116)
12. Wainwright P, Kraklau D, Bennet A. 1991 Kinematics of tongue projection in *Chamaeleo oustaleti*. *J. Exp. Biol.* **159**, 109–133.
13. Patek S, Nowroozi B, Baio J, Caldwell R, Summers A. 2007 Linkage mechanics and power amplification of the mantis shrimp's strike. *J. Exp. Biol.* **210**, 3677–3688. (doi:10.1242/jeb.006486)
14. Peplowski M, Marsh R. 1997 Work and power output in the hindlimb muscles of Cuban tree frogs *Osteopilus septentrionalis* during jumping. *J. Exp. Biol.* **200**, 2861–2870.
15. Sutton G, Burrows M. 2011 Biomechanics of jumping in the flea. *J. Exp. Biol.* **214**, 836–847. (doi:10.1242/jeb.052399)
16. Patek S. 2015 The most powerful movements in biology. *AM Sci.* **103**, 330. (doi:10.1511/2015.116.330)
17. McGowan C, Baudinette R, Usherwood J, Biewener A. 2005 The mechanics of jumping versus steady hopping in yellow-footed rock wallabies. *J. Exp. Biol.* **208**, 2741–2751. (doi:10.1242/jeb.01702)
18. Burrows M, Shaw S, Sutton G. 2008 Resilin and chitinous cuticle form a composite structure for energy storage in jumping by froghopper insects. *BMC Biol.* **6**, 41. (doi:10.1186/1741-7007-6-41)
19. Benjamin SP, Zschokke S. 2002 Untangling the tangle-web: web construction behavior of the comb-footed spider *Steatoda triangulosa* and comments on phylogenetic implications (Araneae: Theridiidae). *J. Insect Behav.* **15**, 791–809. (doi:10.1023/A:1021175507377)
20. Argintean S, Chen J, Kim M, Moore AMF. 2006 Resilient silk captures prey in black widow cobwebs. *Appl. Phys. A.* **82**, 235–241. (doi:10.1007/s00339-005-3430-y)
21. Nyffeler BM, Dean DA, Sterling WL. 1988 The southern black widow spider, *Latrodectus rnactans* (Araneae, Theridiidae), as a predator of the red imported fire ant, *Solenopsis invicta* (Hymenoptera, Formicidae), in Texas cotton fields. *J. Appl. Entomol.* **106**, 52–57. (doi:10.1111/j.1439-0418.1988.tb00563.x)
22. Vasanthavada K *et al*. 2012 Spider glue proteins have distinct architectures compared with traditional spidroin family members. *J. Biol. Chem.* **287**, 35 985–35 999. (doi:10.1074/jbc.M112.399816)
23. Choresh O, Bayarmagnai B, Lewis RV. 2009 Spider web glue: two proteins expressed from opposite strands of the same DNA sequence. *Biomacromolecules* **10**, 2852–2856. (doi:10.1021/bm900681w)
24. Ewing HE. 1918 The life and behavior of the house spider. *Proc. Iowa Acad. Sci.* **25**, 177–204.
25. Nyffeler M, Vetter RS. 2018 Black widow spiders, *Latrodectus* spp. (Araneae: Theridiidae), and other spiders feeding on mammals. *J. Arachnol.* **46**, 541–548. (doi:10.1636/JoA-S-18-026.1)
26. Davis DR, Farkas JK, Kerby JL, Dahlhoff MW. 2017 *Coluber constrictor* (North American racer). Predation. Natural history notes. *Herpetol. Rev.* **48**, 446–447.
27. McCook HC. 1889 *American spiders and their spinning work. A natural history of the orbweaving spiders of the United States, with special regard to their industry and habits*. Philadelphia, PA: Academy of Natural Sciences of Philadelphia.
28. McKeown KC. 1944 Proceedings of the Royal Zoological Society of New South Wales for the year 1943-44. See http://www.biodiversitylibrary.org/item/119540.
29. Bigot L. 1969 Sur le comportement en captivitè de l'araignee Olios coenobita Fage. *C R Hebd Seance Acad. Sci.* **D 268**, 729–730.
30. Decary R. 1918 Notes concernant les moeurs de deux curieuses espèces d'araignées observées dans le sud de l'île. *Bull Acad Malgache N S IV.* **4**, 20–21.
31. Decary R. 1926 Observations sur l' Olios coenobita Fage et le Nemoscolus waterloti Berland. *Arch. Zool. Exp. Gen.* **65**, 18–21.

32. Foelix VR, Thieleczek R, Erb B. 2019 Spinnen in Schneckenhäusern: Wie bringen sie ihre Schalen in luftige Höhen? *ARACHNE*. **24**, 1–10.
33. Decary M. 1918 Colonie de madagascab et dependances nouvelle serie. *Bullettin de l'Academie Malgache.* **IV**, 20–21.
34. Fage L. 1926 Sur quelques Araignées de Madagascar, nouvelles ou peu connues et sur leur curieuse industrie. *Arch. Zool. Expr. Gen.* **65**, 5–17.
35. Pugno NM. 2018 Spider weight dragging and lifting mechanics. *Meccanica* **53**, 1105–1114. (doi:10.1007/s11012-017-0787-x)
36. Blackledge TA, Cardullo RA, Hayashi CY. 2005 Polarized light microscopy, variability in spider silk diameters, and the mechanical characterization of spider silk. *Invertebr. Biol.* **124**, 165–173. (doi:10.1111/j.1744-7410.2005.00016.x)
37. Schneider CA, Rasband WS, Eliceri KW. 2012 NIH Image to ImageJ: 25 years of image analysis. *Nat. Methods.* **9**, 671–675. (doi:10.1038/nmeth.2089)
38. Foelix R. 2011 *Biology of spiders*. London, UK: Oxford University Press.
39. Benjamin SP, Zschokke S. 2003 Webs of theridiid spiders: construction, structure and evolution. *Biol. J. Linn. Soc.* **78**, 293–305. (doi:10.1046/j.1095-8312.2003.00110.x)
40. Blackledge TA, Coddington JA, Gillespie RG. 2003 Are three-dimensional spider webs defensive adaptations? *Ecol. Lett.* **6**, 13–18. (doi:10.1046/j.1461-0248.2003.00384.x)
41. Greco G, Pantano MF, Mazzolai B, Pugno NM. 2019 Imaging and mechanical characterization of different junctions in spider orb webs. *Sci. Rep.* **9**, 5776. (doi:10.1038/s41598-019-42070-8)
42. Blackledge TA. 2005 Quasistatic and continuous dynamic characterization of the mechanical properties of silk from the cobweb of the black widow spider *Latrodectus hesperus*. *J. Exp. Biol.* **208**, 1937–1949. (doi:10.1242/jeb.01597)
43. Sahni V, Harris J, Blackledge TA, Dhinojwala A. 2012 Cobweb-weaving spiders produce different attachment discs for locomotion and prey capture. *Nat. Commun.* **3**, 1106–1107. (doi:10.1038/ncomms2099)
44. Greco G, Wolff J, Pugno NM. 2020 Strong and tough silk for resilient attachment discs: the mechanical properties of piriform silk, in the spider *Cupiennius salei* (Keyserling, 1877). *Front. Mater.* **7**, 138. (doi:10.3389/fmats.2020.00138)
45. Blackledge TA, Summers AP, Hayashi CY. 2005 Gumfooted lines in black widow cobwebs and the mechanical properties of spider capture silk. *Zoology* **108**, 41–46. (doi:10.1016/j.zool.2004.11.001)
46. Hayashi CY, Blackledge TA, Lewis RV. 2004 Molecular and mechanical characterization of aciniform silk: uniformity of iterated sequence modules in a novel member of the spider silk fibroin gene family. *Mol. Biol. Evol.* **21**, 1950–1959. (doi:10.1093/molbev/msh204)
47. Hennecke K, Redeker J, Kuhbier JW, Strauss S, Allmeling C, Kasper C, Reimers K, Vogt PM. 2013 Bundles of spider silk, braided into sutures, resist basic cyclic tests: potential use for flexor tendon repair. *PLoS ONE* **8**, e61100. (doi:10.1371/journal.pone.0061100)
48. Kumar B, Singh KP. 2014 Fatigueless response of spider draglines in cyclic torsion facilitated by reversible molecular deformation. *Appl. Phys. Lett.* **105**, 10–15.
49. Vehoff T, Glišović A, Schollmeyer H, Zippelius A, Salditt T. 2007 Mechanical properties of spider dragline silk: humidity, hysteresis, and relaxation. *Biophys. J.* **93**, 4425–4432. (doi:10.1529/biophysj.106.099309)
50. Sampath S, Yarger JL. 2015 Structural hysteresis in dragline spider silks induced by supercontraction: an X-ray fiber micro-diffraction study. *RSC Adv.* **5**, 1462–1473. (doi:10.1039/C4RA13936D)
51. Gosline JM, Guerette PA, Ortlepp CS, Savage KN. 1999 The mechanical design of spider silks: from fibroin sequence to mechanical function. *J. Exp. Biol.* **202**, 3295–3303.

Supplementary information

How spiders hunt heavy prey: the tangle web as a pulley and spider's lifting mechanics observed and quantified in the laboratory

Gabriele Greco [1], Nicola M. Pugno [1, 2*]

[1] Laboratory of Bio-Inspired, Bionic, Nano, Meta Materials & Mechanics, Department of Civil, Environmental and Mechanical Engineering, University of Trento, Via Mesiano, 77, 38123 Trento, Italy

[2] School of Engineering and Materials Science, Queen Mary University of London, Mile End Road, E1 4NS London, United Kingdom

*Corresponding author: nicola.pugno@unitn.it

The mechanical model (detailed description)

Linear regime I strategy

Following Figure 2 we wrote the vertical force equilibrium between the weight of the prey and the overall vertical component of the tension generated by the threads for each lifting's step[21]:

1) $\frac{W}{A} = \sum_{i=1}^{N_I} \sigma_{i1} \cos\theta_{i1} + \sigma_{11} \cos\theta_{11} = \sum_{i=1}^{N_I} \left(E\left(\frac{l_{i1}}{l_0} - 1\right) \cos\theta_{i1} \right) + \cos\theta_{11}\, E\left(\frac{l_{11}}{l_0} - 1\right) =$

$\sum_{i=1}^{N_I} \left(E\left(\frac{y_1}{\cos\theta_{i1}\, l_0} - 1\right) \cos\theta_{i1} \right) + \cos\theta_{11}\, E\left(\frac{y_1}{\cos\theta_{11}\, l_0} - 1\right)$

$$\Rightarrow y_1 = \frac{l_0}{E(N_I + 1)} \left(\frac{W}{A} + E \sum_{i=1}^{N_I} \cos\theta_{i1} + E \cos\theta_{11} \right)$$

where A is the cross-sectional area of the silk thread (considered constant during the process) and y_i is the vertical distance between the prey and the anchorage of the thread. The first sum (till N_I) of vertical components of the threads' tensions was related to the silk fibres inserted prior to lifting. The next step was described as follow[21]:

2) $\frac{W}{A} = \sum_{i=1}^{N_I} \sigma_{i2} \cos\theta_{i2} + \sigma_{12} \cos\theta_{12} + \sigma_{22} \cos\theta_{22} = \sum_{i=1}^{N_I} \left(E\left(\frac{l_{i2}}{l_0} - 1\right) \cos\theta_{i2} \right) +$

$\cos\theta_{12}\, E\left(\frac{l_{12}}{l_0} - 1\right) + \cos\theta_{22}\, E\left(\frac{l_{22}}{l_0} - 1\right) = \sum_{i=1}^{N_I} \left(E\left(\frac{y_2}{\cos\theta_{i2}\, l_0} - 1\right) \cos\theta_{i2} \right) +$

$+ \cos\theta_{12}\, E\left(\frac{y_2}{\cos\theta_{12}\, l_0} - 1\right) + + \cos\theta_{22}\, E\left(\frac{y_2}{\cos\theta_{22}\, l_0} - 1\right)$

$$\Rightarrow y_2 = \frac{l_0}{E(N_I + 2)} \left(\frac{W}{A} + E \sum_{i=1}^{N_I} \cos\theta_{i2} + E(\cos\theta_{12} + \cos\theta_{22}) \right)$$

…

n) $y_n = \frac{l_0}{E(N_I + n)} \left(\frac{W}{A} + E \sum_{i=1}^{N_I} \cos\theta_{in} + E \sum_{i=1}^{n} \cos\theta_{in} \right)$

If the height of the anchorages is constant during the process, we calculated the height of the prey at the lifting's step *n* by using[21]:

$$H_n = y_0 - y_n = y_0 - \frac{l_0}{E(N_I + n)}\left(\frac{W}{A} + E\sum_{i=1}^{N_I}\cos\theta_{in} + E\sum_{i=1}^{n}\cos\theta_{in}\right) \quad (1)$$

Linear regime II strategy

We proceed by following the previous logic scheme. However, this time the length l_0 was not known but the overall strain of all the threads at each step *j* was known (ε_j). Again, we analysed step by step and thus we obtained[21]:

1) $\frac{W}{A} = \sum_{i=1}^{N_I}\sigma_{i1}\cos\theta_{i1} + \sigma_{11}\cos\theta_{11} = \sum_{i=1}^{N_I} E\cos\theta_{i1}\left(\frac{l_{i1}}{l_{i0}} - 1\right) + E\cos\theta_{11}\left(\frac{l_{11}}{l_{10}} - 1\right) =$

$\sum_{i=1}^{N_I}\frac{Ey_1}{l_{i1}}(1+\varepsilon_1) - E\sum_{i=1}^{N_I}\cos\theta_{i1} + \frac{Ey_1}{l_{11}}(1+\varepsilon_1) - E\cos\theta_{11}$

$$\Rightarrow y_1 = \frac{1}{E(1+\varepsilon_1)}\left(\frac{W}{A} + E\left(\sum_{i=1}^{N_I}\cos\theta_{i1} + \cos\theta_{11}\right)\right)\left(\sum_{i=1}^{N_I}\frac{1}{l_{i1}} + \frac{1}{l_{11}}\right)^{-1}$$

where first sum (till N_I) of vertical components of the threads' tensions is related to the silk fibres inserted prior to lifting. The next step is described as follow[21]:

2) $\frac{W}{A} = \sum_{i=1}^{N_I}\sigma_{i2}\cos\theta_{i2} + \sigma_{12}\cos\theta_{12} + \sigma_{22}\cos\theta_{22} = \sum_{i=1}^{N_I} E\cos\theta_{i2}\left(\frac{l_{i2}}{l_{i0}} - 1\right) +$

$E\cos\theta_{12}\left(\frac{l_{12}}{l_{10}} - 1\right) + E\cos\theta_{22}\left(\frac{l_{22}}{l_{20}} - 1\right) = \sum_{i=1}^{N_I}\frac{Ey_2}{l_{i2}}(1+\varepsilon_2) - E\sum_{i=1}^{N_I}\cos\theta_{i2} + \frac{Ey_2}{l_{12}}(1+$

$\varepsilon_2) - E\cos\theta_{12} + \frac{Ey_2}{l_{22}}(1+\varepsilon_2) - E\cos\theta_{22}$

$$\Rightarrow y_2 = \frac{1}{E(1+\varepsilon_2)}\left(\frac{W}{A} + E\left(\sum_{i=1}^{N_I}\cos\theta_{i2} + \cos\theta_{12} + \cos\theta_{22}\right)\right)\left(\sum_{i=1}^{N_I}\frac{1}{l_{i2}} + \frac{1}{l_{12}} + \frac{1}{l_{22}}\right)^{-1}$$

…

n) $y_n = \frac{1}{E(1+\varepsilon_n)}\left(\frac{W}{A} + E\left(\sum_{i=1}^{N_I}\cos\theta_{in} + \sum_{i=1}^{n}\cos\theta_{in}\right)\right)\left(\sum_{i=1}^{N_I}\frac{1}{l_{in}} + \sum_{i=1}^{n}\frac{1}{l_{in}}\right)^{-1}$

If the height of the anchorages is constant during the process, we can compute the height of the prey at the lifting's step *n* by using[21]:

$$H_n = y_0 - \frac{1}{E(1+\varepsilon_n)}\left(\frac{W}{A} + E\left(\sum_{i=1}^{N_I}\cos\theta_{in} + \sum_{i=1}^{n}\cos\theta_{in}\right)\right)\left(\sum_{i=1}^{N_I}\frac{1}{l_{in}} + \sum_{i=1}^{n}\frac{1}{l_{in}}\right)^{-1} \quad (2)$$

Nonlinear regime II strategy

For the sake of simplicity, we do not consider the I strategy for the nonlinear regimes.

Following the previous logic and the process step by step we obtained[21]:

1) $\frac{W}{A} = \sum_{i=1}^{N_I} \sigma_{i1} \cos\theta_{i1} + \sigma_{11}\cos\theta_{11} = \sum_{i=1}^{N_I} \cos\theta_{i1} \frac{\sigma_u}{\varepsilon_u^\alpha} \ln^\alpha\left(\frac{l_{i1}}{l_{i0}}\right) + \cos\theta_{11} \frac{\sigma_u}{\varepsilon_u^\alpha} \ln^\alpha\left(\frac{l_{11}}{l_{10}}\right) =$

$\sum_{i=1}^{N_I} \frac{y_1}{l_{i1}} \frac{\sigma_u}{\varepsilon_u^\alpha} \ln^\alpha(1+\varepsilon_1) + \frac{y_1 \sigma_u}{l_{11}\varepsilon_u^\alpha} \ln^\alpha(1+\varepsilon_1)$

$$\Rightarrow y_1 = \frac{W}{A} \frac{\varepsilon_u^\alpha}{\sigma_u} \frac{1}{\ln^\alpha(1+\varepsilon_1)} \left(\sum_{i=1}^{N_I} \frac{1}{l_{i1}} + \frac{1}{l_{11}} \right)^{-1}$$

where first sum (till N_I) of vertical components of the threads' tensions was related to the silk fibres inserted prior to lifting. The next step was described as follow[21]:

2) $\frac{W}{A} = \sum_{i=1}^{N_I} \sigma_{i2} \cos\theta_{i2} + \sigma_{12}\cos\theta_{12} + \sigma_{22}\cos\theta_{22} = \sum_{i=1}^{N_I} \cos\theta_{i2} \frac{\sigma_u}{\varepsilon_u^\alpha} \ln^\alpha\left(\frac{l_{i2}}{l_{i0}}\right) +$

$\cos\theta_{12} \frac{\sigma_u}{\varepsilon_u^\alpha} \ln^\alpha\left(\frac{l_{12}}{l_{10}}\right) + \cos\theta_{22} \frac{\sigma_u}{\varepsilon_u^\alpha} \ln^\alpha\left(\frac{l_{22}}{l_{20}}\right) = \sum_{i=1}^{N_I} \frac{y_2}{l_{i2}} \frac{\sigma_u}{\varepsilon_u^\alpha} \ln^\alpha(1+\varepsilon_2) + \frac{y_2 \sigma_u}{l_{12}\varepsilon_u^\alpha} \ln^\alpha(1+\varepsilon_2) +$

$\frac{y_2 \sigma_u}{l_{22}\varepsilon_u^\alpha} \ln^\alpha(1+\varepsilon_2)$

$$\Rightarrow y_2 = \frac{W}{A} \frac{\varepsilon_u^\alpha}{\sigma_u} \frac{1}{\ln^\alpha(1+\varepsilon_2)} \left(\sum_{i=1}^{N_I} \frac{1}{l_{i2}} + \frac{1}{l_{12}} + \frac{1}{l_{22}} \right)^{-1}$$

…

n) $y_n = \frac{W}{A} \frac{\varepsilon_u^\alpha}{\sigma_u} \frac{1}{\ln^\alpha(1+\varepsilon_n)} \left(\sum_{i=1}^{N_I} \frac{1}{l_{in}} + \sum_{i=1}^{n} \frac{1}{l_{in}} \right)^{-1}$

If the height of the anchorages is constant during the process, we can compute the height of the prey at the lifting's step *n* by using[21]:

$$H_n = y_0 - \frac{W}{A} \frac{\varepsilon_u^\alpha}{\sigma_u} \frac{1}{\ln^\alpha(1+\varepsilon_n)} \left(\sum_{i=1}^{N_I} \frac{1}{l_{in}} + \sum_{i=1}^{n} \frac{1}{l_{in}} \right)^{-1} \qquad (3)$$

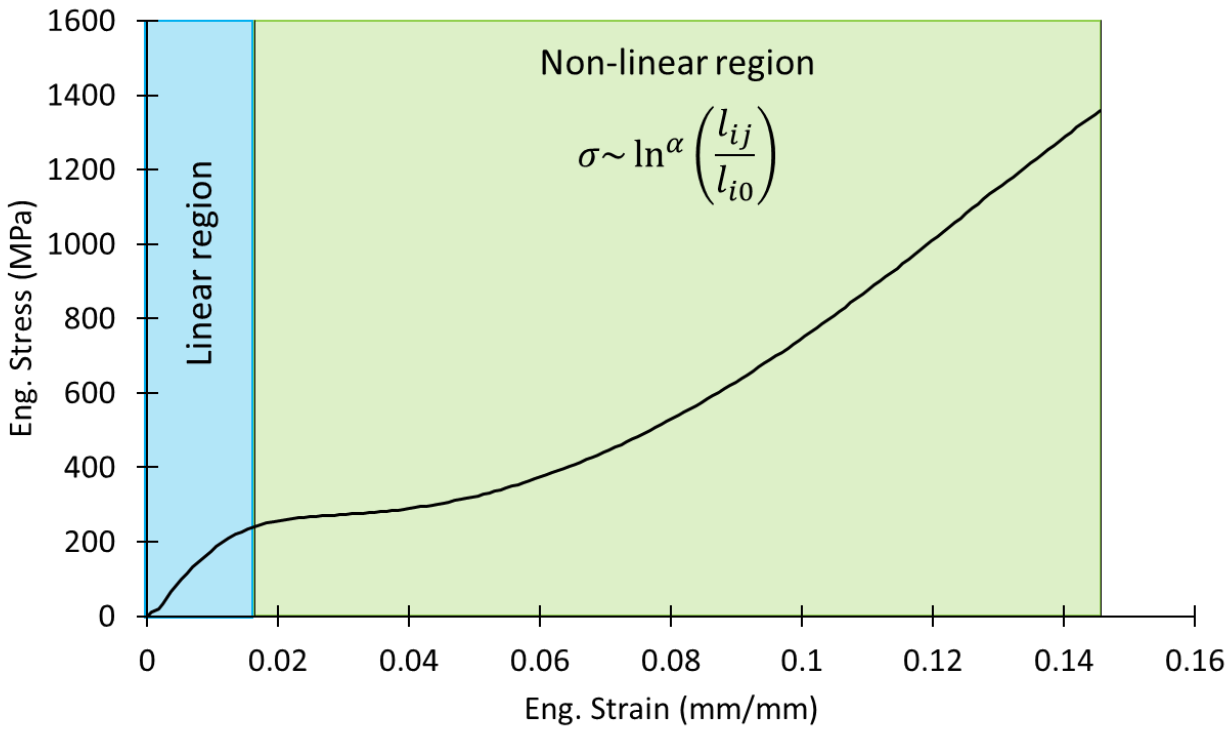

Figure S1: A typical stress strain curve of a spider silk fibre. In order to compute α, we fit the nonlinear region with the indicated equation. The first region, on the other hand, is the linear one.

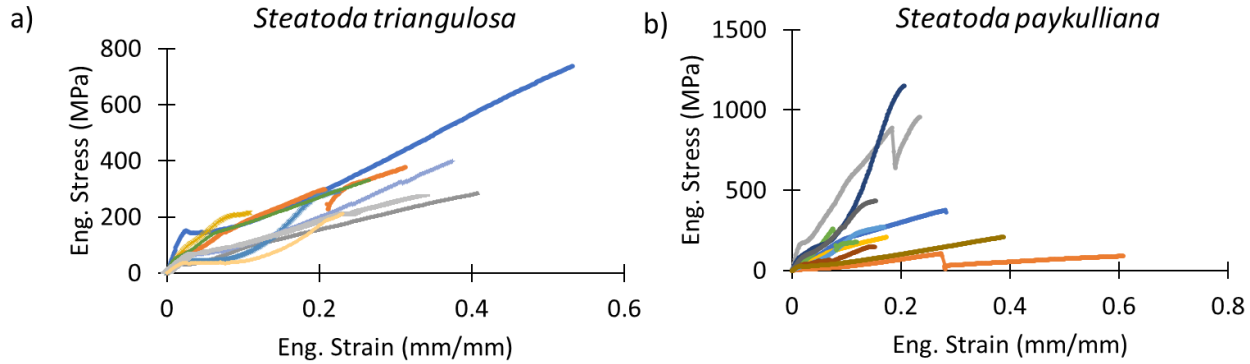

Figure S2: The mechanical properties of the catching thread (without glue) of the two species of spiders that were studied. a) Stress-strain curves of the species Steatoda triangulosa, b) stress-strain curves of the species Steatoda paykulliana.

Table S1: The number of threads used (whole process) to lift the prey, their mean length and the final height at which the prey is lifted at the end of the process. N_I is the number of threads inserted prior the lifting and n is the number of threads inserted during the lifting.

Spider	Number of used threads		Final Height (cm)
	N_I	n	
Steatoda triangulosa 1°	5	24	5.70 ± 2.39
Steatoda triangulosa 2°	13	60	4.30 ± 2.07
Steatoda triangulosa 3°	11	36	3.00 ± 1.73
Steatoda triangulosa 4°	3	31	5.40 ± 2.3
Steatoda paykulliana	13	4	0.80 ± 0. 35

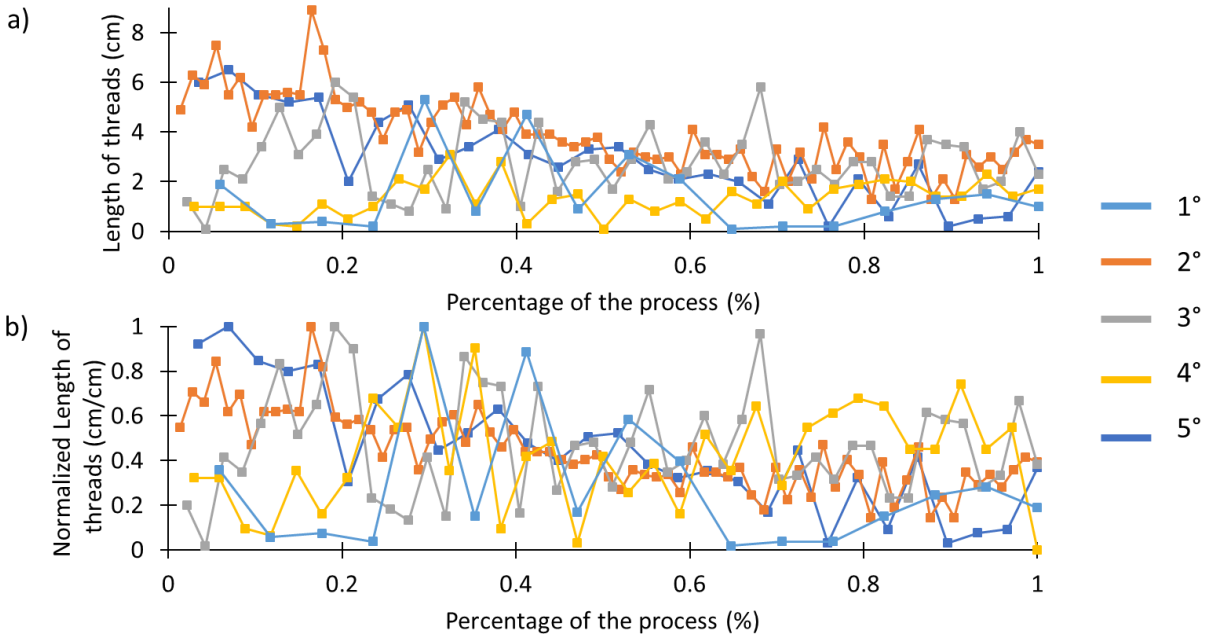

Figure S3: a) Length of the inserted threads vs the step of the lifting mechanisms (express in percentage). b) Normalized length of the thread (with respect to the longest) vs the step of the lifting mechanism (expressed in percentage). No particular regularity is observed. The percentage of the process means the state of the hunt with respect to its end (i.e. when the spider stops to spin). It is simply computed by dividing the number of the actual step (i.e. the number of the inserted fibres) for the total number of steps.

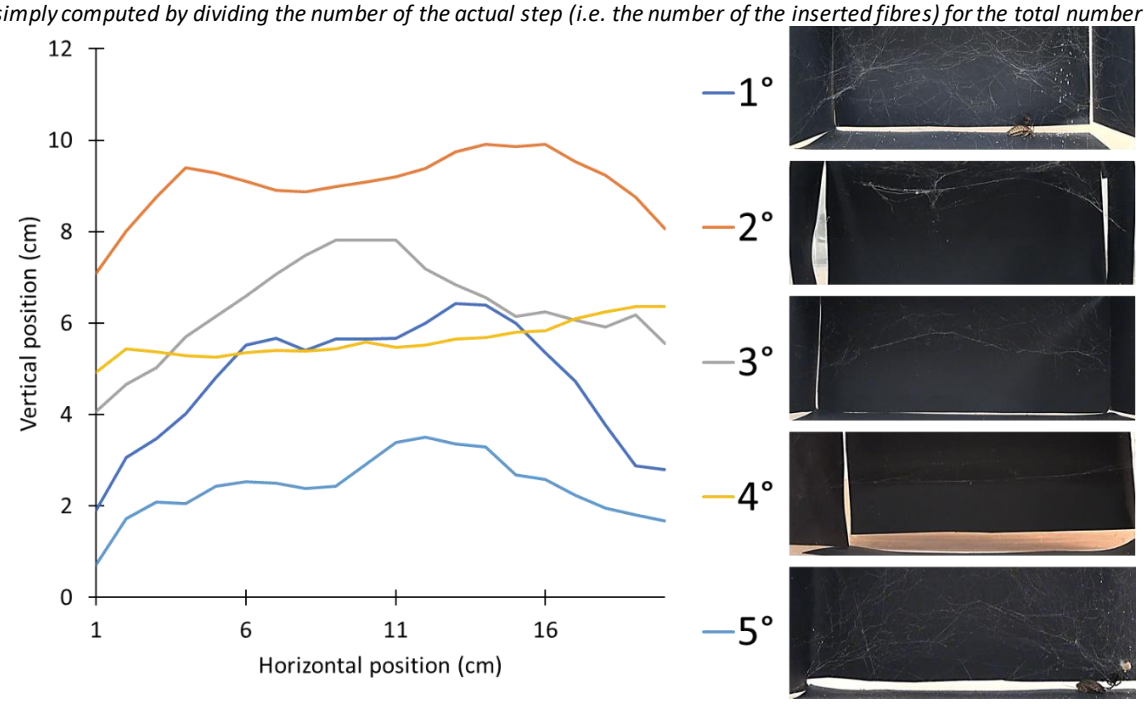

Figure S4: The height profile of the main structure of the tangle webs of the tested spiders.

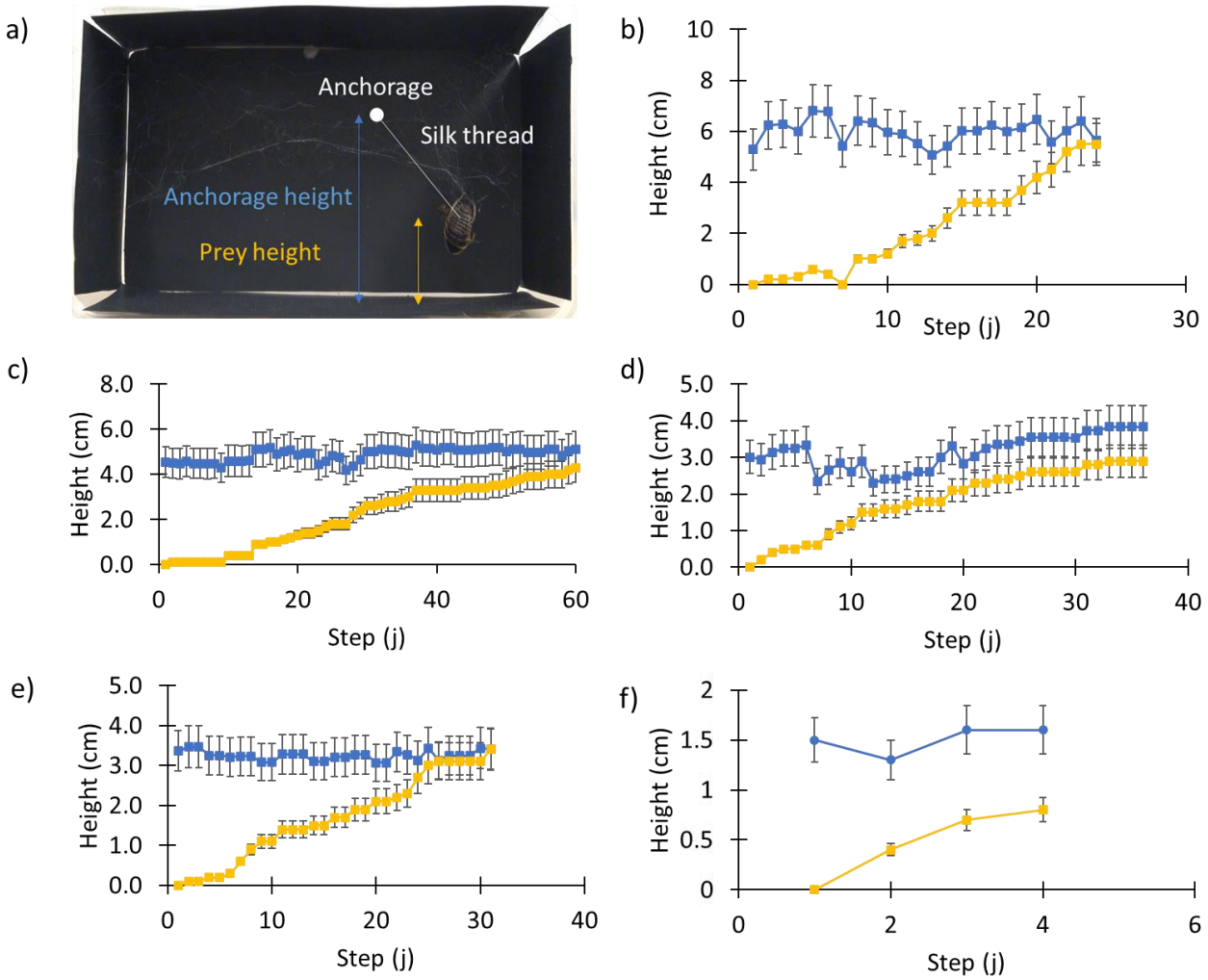

Figure S5: a) Comparison between the height of the prey and the height of the anchorages during the process. Notice the almost constant height of the anchorages during the predation of the analysed spiders: b) Steatoda triangulosa 1°, c) Steatoda triangulosa 2°, d) Steatoda triangulosa 3°, e) Steatoda triangulosa 4° and f) Steatoda paykulliana.

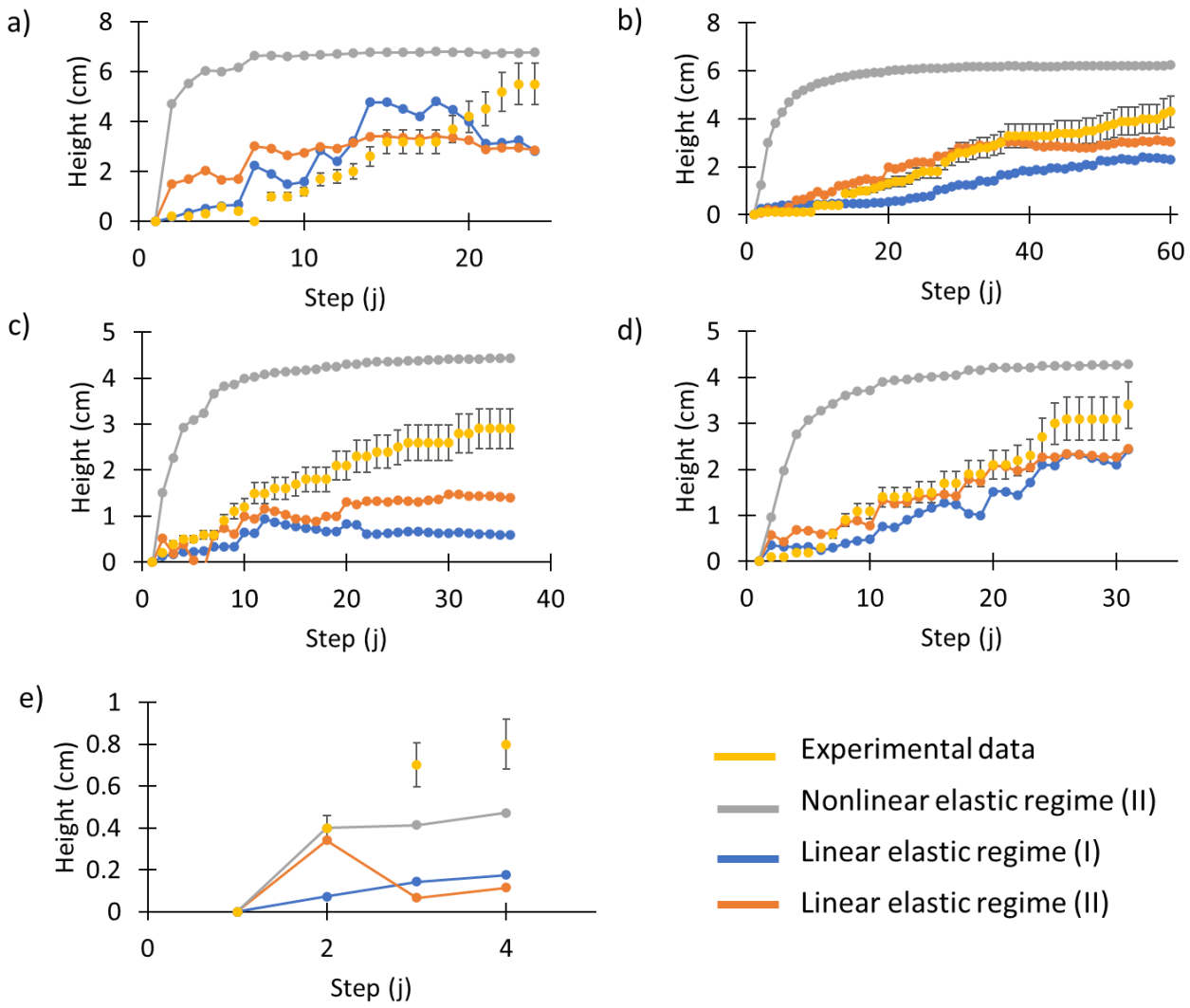

Figure S6: Comparison among the theoretical model and the experimental data of the lifting of Steatoda triangulosa 1° (a), 2° (b), 3° (c), 4° (d). e) Comparison among the mix-model and the experimental data of the lifting of Steatoda paykulliana. Grey lines = nonlinear elastic regime (II strategy); blue lines = linear elastic regime (I strategy); orange line = linear elastic regime (II strategy); yellow points = experimental data.